Structural and Dynamic Approach of Early Hydration Steps in Erodable Polymers by ATR−FTIR and Fluorescence Spectroscopies

Muriel Thouvenin,[†] Isabelle Linossier,[‡] Olivier Sire,[†] Jean-Jacques Péron,[†] and Karine Vallée-Réhel*[,†]

Laboratoire de Biologie et Chimie Moléculaires and Laboratoire Polymères et Procédés, Université de Bretagne-Sud, Rue Saint-Maudé, BP 92116, 56321 Lorient, France

Received March 22, 2001; Revised Manuscript Received September 19, 2001

ABSTRACT: The understanding of mechanisms involved in the controlled release of active molecules from the polymer matrix requires the study of hydration phenomenon. Fluorescence and attenuated total reflection Fourier transform infrared (ATR−FTIR) spectroscopies were used to analyze the earlier steps of hydration in acrylic copolymers. The effect of hydration on the anisotropy of the PRODAN fluorescent probe showed a change in the dynamics of the macromolecular chains. By using ATR−FTIR spectroscopy, the structure of dissolved water in polymers was studied. The evolution of this structure was performed as hydration proceeds by band decomposition of the ν_{OH} vibration on the basis of the four-state model which allows discriminating bound from free molecules: in the "early" stages of hydration, the water network appears drastically perturbed as compared to that of bulk pure water, this perturbation vanishing in the "later" stages of hydration. Besides, this study reveals that the polymer carbonyl groups constitutes the major water binding sites as it was deduced from their progressive engagement in H bonds in the time course of hydration. The rate and extent of this process was observed to be correlated with the hydrophobicity of polymers. The present findings, obtained on similar time scales from noninvasive techniques, indicate that both dynamic and structural consequences of hydration are correlated in most of the polymers here studied.

Introduction

In recent years, much work has focused on the development of controlled release devices. Polymers for sustained release of biologically active molecules were first developed in the biomedical field, but today they are also used in many areas, particularly in the environmental domain. Applications mostly concern agriculture (fungicides, insecticides, fertilizers) and navigation (antifouling paints).[1]

These delivery systems provide release rates, which are determined by the physical properties of the device itself. Different forms are used, such as hydrogels, liposomes, micelles, and nanoparticles. The objective is to increase the efficiency of the release of the entrapped molecules, its targeting toward specific cells and the reduction of its toxicity. Many mechanisms are proposed to explain the release of the molecules: surface erosion, simple diffusion or diffusion coupled with bulk erosion, and dissolution, swelling, or entrapping effects of solute molecules inside the polymer matrix.[2,3] In all cases, matrix hydration is essential and needs to be controlled. The design of erodable systems also requires the understanding of both erosion and hydrolytic degradation processes.

Research works published so far on polymers hydration approach this phenomenon by both the qualitative and quantitative ways. The main properties studied are the absorbed water amount (by gravimetric methods), the various classes of water diffusion kinetics (Fickian or non-Fickian behaviors), the forms of absorbed water (bound, free, and clusters), the water localization (identification of hydrated functions in the polymer matrix), and the effects of hydration on structural and dynamic properties of macromolecular chains.[4]

In the present study, the hydration characteristics of five polymers are analyzed. These polymers (Figure 1) were chosen in reference to previous works on their hydrolytic degradation and global hydration:[5,6]

- An organotin copolymer (POS) which associates methyl methacrylate and tributyltin methacrylate monomeric units.
- A blending **(**PAC**)** of acrylic copolymer poly(methyl methacrylate-*co*-butyl methacrylate) with a small organic molecule: rosin (mixture of abietic and dehydroabietic acids).
- Three copolymers which associated hydrophilic, hydrophobic, and hydrolyzable monomeric units by random copolymerization. These monomer units were chosen for the versatility of copolymers obtained due to the possibility of varying the chemical structure of the lateral ester groups: TER2 (poly(trichlorophenyl acrylate-*co*-tertiobutyl acrylate-*co*-dimethylaminoethyl methacrylate)), TER1 (poly(hydroxypropyl acrylate-*co*-tertiobutyl acrylate-*co*-dimethylaminoethyl methacrylate)), PLAtBu (polymethacrylate of oligolactide-*co*-*tert*-butyl acrylate).

The selected polymers possess one common point except the acrylic structure: the ability to release active molecules. Though they exhibit similar release rates of organic (pesticides) or mineral chemicals, they differ in many characteristics: global hydration, degradation kinetics, type of erosion, and mechanical properties. POS and PAC are erodable polymers that keep film properties without absorbing large amounts of water. After six months of immersion, their water uptakes are about 1% (in mass) and their degradation kinetics are

* To whom all correspondence should be addressed.
[†] Laboratoire de Biologie et Chimie Moléculaires.
[‡] Laboratoire Polymères et Procédés.

10.1021/ma010501k CCC: $22.00
Published on Web 12/18/2001

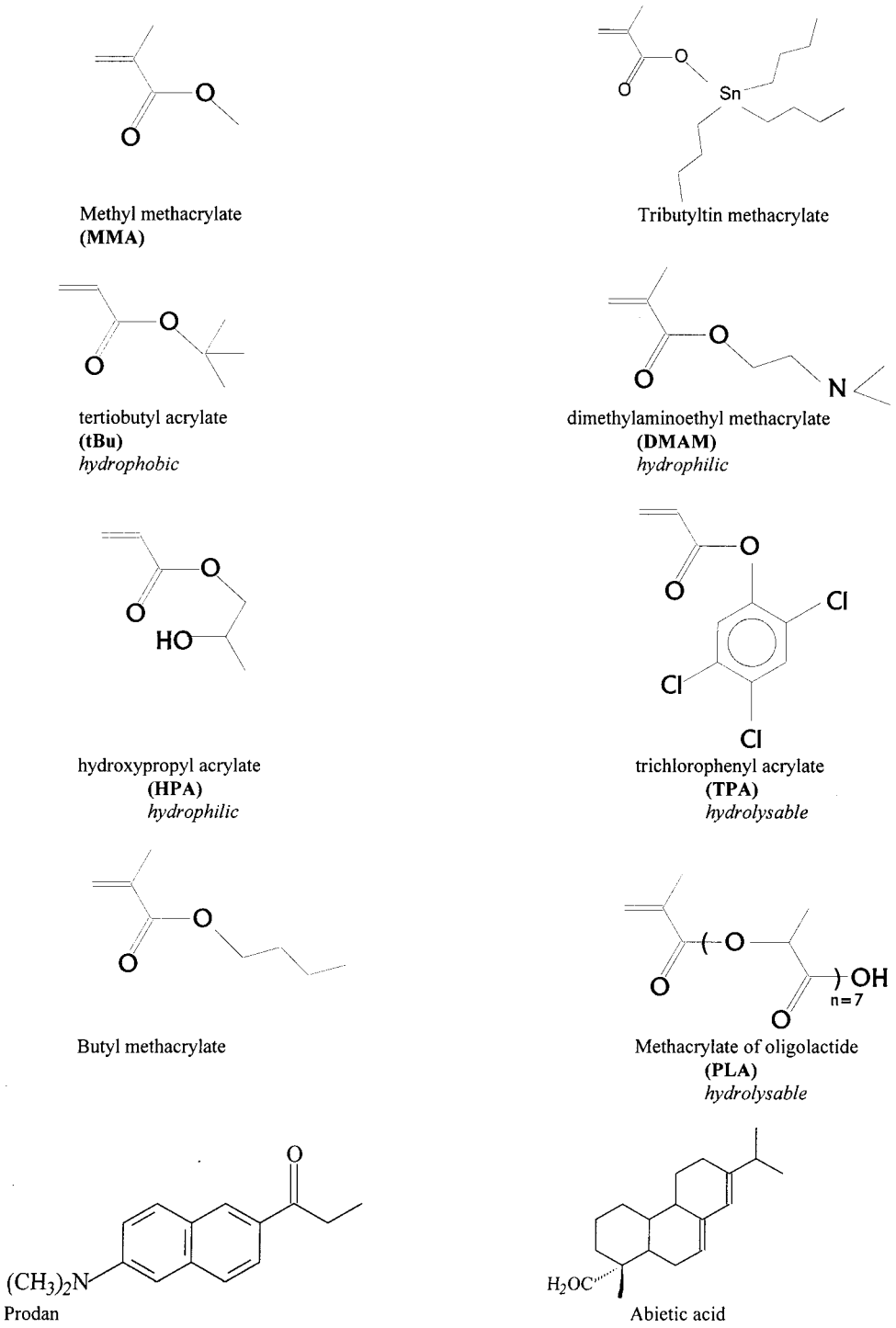

Figure 1. Chemical structure of monomers and PRODAN.

very slow. On opposite, degradation of the three polymers exhibiting various hydrophilic/hydrophobic balances (TER1, TER2, and PLAtBu) requires a significant hydration before degrading (about 10% in mass after 1 month of immersion). Among the five polymers, only POS is likely to undergo surface erosion.

Previous works on hydrolytic degradation of TER1, TER2, and PLAtBu have pointed out the complexity of hydrolysis within or close to the macromolecular chains. The nature of bonds (ester, anhydride, or amide) mainly determines the hydrolysis rate, but rankings must be viewed with circumspection. Reactivities are dependent on the mode of catalysis, on the chemical neighborhood of the affected functional group through steric and electronic effects, or on the amount of bounded water available for hydrolysis reaction.[7,8] It is therefore difficult to classify the reactivity of ester functions from the corresponding low molecular weight compounds (the monomers) containing the same functional group. This complexity underlines the necessity of a better understanding of the first step of hydrolysis, i.e., hydration.

In the present study, hydration during the first time of immersion is analyzed in order to identify some mechanisms of hydration, the water structure in relation to a particular bonding scheme and the resulting effects on the dynamic properties of the various polymer matrixes.

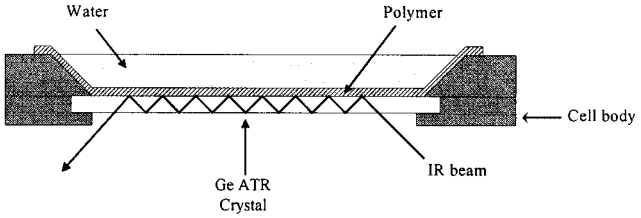

Figure 2. Cell body thermostated ATR accessory.

Experimental Section

Materials. *tert*-Butyl acrylate (tBu), dimethylaminoethyl methacrylate (DMAM), and hydroxypropyl acrylate (HPA) are commercial (Acros Chimica and Interchim). They were distilled before use. Trichlorophenylacrylate was obtained by reaction of acryloyl chloride on the 2,4,5-trichlorophenol.[9] Racemic oligolactic acid was obtained from Phusis SA (France).

Copolymerizations (TER1 and TER2)[6] were carried out in anhydrous dioxane at 70 °C during 24 h using AIBN (1% molar) as initiator. Copolymers were recovered by precipitation in water or petroleum ether and dried in a vacuum at 60 °C.

The methacrylate of lactic acid oligomers was prepared by condensation between methacrylic acid and oligolactic acid in anhydrous CH_2Cl_2 with DCC and DMAP.[10]

Polymers were dissolved in xylene or THF (50% weight) and applied with a filmograph (thickness of the dry film: 100 μm) on a polycarbonate sheet. The solvent was allowed to evaporate.

Methods. Fourier transform infrared spectroscopy (FTIR) of anhydrous and hydrated polymers was performed in the attenuated total reflection (ATR) mode by using a Nicolet FTIR 460 Protege (Thermo Optek) equipped with a DTGS detector and a thermostated ATR accessory (Figure 2). Solubilized copolymers were applied onto a Ge 45° ATR crystal (Spectra-Tech) and were allowed to dry under vacuum for 2 h. Then, the layered crystal (about 100 μm thick) was placed in a desiccator, evacuated for 3 h and allowed to equilibrate for at least 1 day. A first FTIR−ATR spectrum was collected under "anhydrous" conditions; then water was added in excess, and "hydrated" spectra were sequentially collected for periods up to 100 h. The background was collected and digitally stored before applying the polymer on the optical surface. Spectra result from the accumulation of 256 scans at 2 cm^{-1} resolution. The crystal temperature was set to 25 ± 1 °C. Depending on the overall period of time monitored, the spectra were collected either in a continuous mode or with a time lag of 1 h in order to get a 50−100 spectra data set. Each experiment was repeated at least three times.

Fluorescence experiments were achieved by using the PRODAN 6-propionyl-2-dimethylaminonaphthalene fluorophore (P-248 Molecular Probes) since this probe exhibits Stoke's shifts which sensitively respond to the polarity in its environment. Copolymer labeling were performed by mixing 2 g of the various copolymers, 0.6 mg of the fluorescent probe, and 1 g of xylene or THF. A day later, the solubilized copolymer was applied on a polycarbonate sheet as a 100 μm thick film, and the solvent was allowed to evaporate. Fluorescence emission spectra were collected by using an LS-50B spectrofluorimeter (Perkin-Elmer). A narrow sheet of the copolymer film was cut out to fit the diagonal of a 1 cm × 1 cm quartz cuvette in order to collect the fluorescence emission in the front mode. Excitation and emission slits were set to 2.5 nm. Emission spectra, collected by using an excitation wavelength of 350 nm, are the average of three scans acquired with a 1s integration time and a 1 nm step. Every fluorescence emission spectrum was subtracted for intrinsic fluorescence (arising either from the polycarbonate or the copolymer) by interactively subtracting the signal arising from the corresponding unlabeled copolymer sample. Fluorescence anisotropy experiments were performed to record over 6 h dynamic changes occurring in the probe environment after polymer hydration. Parallel and perpendicular emission components were measured by using the "fast filter wheel" device. Fluorescence intensities were collected at 420 nm. The anisotropy of fluorescence (A) is defined as the difference between the parallel ($I_{||}$) and perpendicular ($I_{\perp}$) emission components with respect to the total intensity when vertically polarized excitation is used:

$$A = \frac{I_{||} - I_{\perp}}{I_{||} + 2I_{\perp}} \tag{1}$$

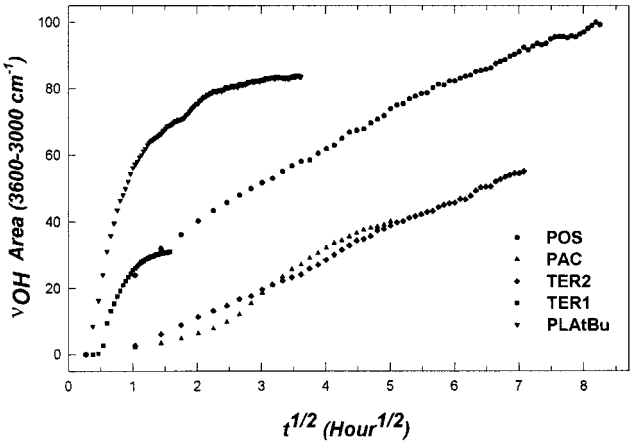

Figure 3. Hydration kinetics. Integrated areas of the water ν_{OH} vibrational band are plotted as a function of $\sqrt{t}$. Infrared spectra have been sequentially collected at 25 °C in the ATR mode with a 2 cm^{-1} resolution. The copolymer initial absorbance in the 3600−3000 cm^{-1} frequency domain was subtracted from every spectrum before integration. The recovered parameters of the kinetics are displayed in Table 1.

Band and Curve Fitting. More detailed analysis of the IR spectra has been achieved by fitting the overall band profiles of the water ν_{OH} and copolymers $\nu_{C=O}$ carbonyl stretching bands. IR spectra were first corrected for ATR-induced distortions due to the wavelength dependent depth of penetration. A refractive index of 1.5 and 1.4 were used for pure water and copolymers spectra, respectively. Then, band decomposition was achieved as previously described[11,12] by identifying the number and approximate location of the underlying spectral components from the second derivative spectra. Then, these parameters were used as "first guess" for performing a nonlinear regression analysis, assuming a mixed Gaussian/Lorentzian shape for the components. Hence, each spectrum was described by four parameters times the number of components plus one for the baseline, which were all allowed to vary upon iteration.

A similar nonlinear regression was achieved to fit infrared hydration and fluorescence anisotropy kinetics. For this purpose, data were fitted as a sum of exponential decays of the form

$$Y_t = \sum_{i=1}^{n} A_i \exp^{-[t/\tau_i]\beta_i} \tag{2}$$

where n, A, τ, and β reflect the number of decays, the amplitude of variation (ν_{OH} area or fluorescence anisotropy), the decay time, and the exponential stretch factor ($0 < \beta \leq 1$), respectively.

Results and Discussion

Kinetics of Hydration. The kinetics of hydration of the five copolymers investigated were studied by using FTIR−ATR spectroscopy to monitor the time-evolution of the water sorbed by the polymer matrix. Figure 3 shows the evolution of the ν_{OH} band area (3600−3000 cm^{-1}) as a function of $\sqrt{t}$ for the five copolymers studied. Clearly, the polymers differ by both the extent and

Table 1. Kinetics of the ν_{OH} Band Area in the Various Copolymers[a]

copolymer	POS	PAC	PLAtBu	TER1	TER2
decay time(s)	$\tau_1 = 29$ min $\tau_2 = 41$ h	$\tau_1 \approx 14$ h "S" shaped	$\tau_1 = 25$ min $\tau_2 = 4.3$ h	$\tau_1 = 20$ min	$\tau_1 = 35$ h
β factor(s)	$\beta_1 = 0.6$ $\beta_2 = 0.8$	$\beta_1 = 1$	$\beta_1 = 0.8$ $\beta_2 = 1$	$\beta_1 = 0.7$	$\beta_1 = 0.9$
A	132	≈ 48	103	40	74
relative area (%)	$A_1 = 26$ $A_2 = 74$	$A_1 = 100$	$A_1 = 76$ $A_2 = 24$	$A_1 = 100$	$A_1 = 100$

[a] The evolutions with time of the ν_{O-H} stretching mode (3600−3000 cm^{-1}) have been fitted in terms of amplitude A, decay time τ, and exponential stretch factor β from eq 2. A β value equal to unity means a pure exponential law, whereas a value close to 0.5 indicates a root time law which matches the Fick diffusion law. Values given for PAC kinetics are only indicative since they are derived from long time approximation.

kinetic law of water uptake. The computed data are summarized in Table 1. POS, PAC, and TER2 clearly do not reach a plateau value over the period monitored. POS exhibits a bimodal kinetic with a first fast component which obeys the $\sqrt{t}$ Fick law and a second slow component which approaches a pure exponential. It is interesting to note that the first law represents 26% of hydration which suggests that this process is saturable. Indeed, one can hypothesize that the first water molecules will bond to a finite number of "free" binding sites of the polymer. This well matches the stretched exponential, which describes a diffusion process of a solute in such a restrictive network.[13,14] The second phase would reflect a distinct phenomenon characterized by a diffusion process mainly based on water−water interactions. The onset of the second phase will therefore be dependent on a threshold concentration of water molecules within the polymer matrix. PAC hydration kinetics exhibits a "S" shape pattern which suggests that the hydration process is initiated by a cooperative process likely based on the early hydration of few sites which occupancy allows further water molecules to diffuse within the matrix. This behavior has been reported.[15−18] It would be not intrinsically distinct from that proposed for the POS, if one accepts that the diffusion of the very first water molecules would be very slow either because of low chain dynamics or due to a very restricted number of transient binding sites. The last copolymer which presents a "slow" water uptake is TER2 in which water sorption obeys a rather pure ($\beta = 0.9$) exponential law with a decay time of 35 h.

On the opposite side, PLAtBu and TER1 reach an equilibrium rather quickly as compared to the three other copolymers since their ν_{OH} areas reach a plateau after 12 and 2 h, respectively. These two polymers are largely affected by the hydration as deduced from their foamy aspects after few hours of immersion. The hydration kinetics of PLA is best described by a two-law model, the first one exhibiting a β factor of 0.8 and the second being a pure exponential. In opposite, TER1 hydration is marked by a fast ($\tau = 20$ min) water uptake with a β factor of 0.7 indicating a behavior close to the Fick mode of diffusion.

Polarity of the Copolymers Matrix. The different kinetic behavior here observed may rely, at least in part, on the different polarities exhibited by the copolymers matrixes. Those differences should arise from distinct hydrophobic/hydrophilic group balances. Hence, the fluorescent probe PRODAN has been chosen to investigate in situ the polarity of the copolymers since this probe exhibits Stokes shifts which vary from ca. 4000 cm^{-1} in benzene up to ca. 9000 cm^{-1} in water.[19,20] Accordingly, the polarity of the various copolymers here studied can be estimated by comparing the observed PRODAN maximal wavelength of emission to those of the probe in various pure solvents. It arises that most of fluorescence emission spectra (data not shown) present a maximum around 420−430 nm (Stokes shifts in the 4800−5300 cm^{-1} range), values close to those observed for PRODAN in chlorobenzene and chloroform. The most surprising effect is that even in the copolymers exhibiting a large water uptake within few hours (PLAtBu and TER1), as deduced from a large swelling, the PRODAN remains in a rather hydrophobic environment and does not interact with water since its Stokes shift is only slightly increased as compared to the anhydrous samples. It must be recalled that, under the experimental conditions used, the PRODAN wavelength of maximal emission in pure water is located around 520 nm ($\Delta\nu = 9340$ cm^{-1}), about 100 nm more than the most *reddish* spectrum here observed (TER1). Hence, it could be concluded that, even in highly hydrated polymers, hydrophobic and hydrophilic phases coexist without mixing. This matches quite well what is observed for biopolymers in which folding is partially entropy-driven, yielding hydrophobic domains from which water or ions are excluded. Such a behavior seems to be supported by preliminary atomic force microscopy experiments (AFM) which revealed structural heterogeneousness on the nanometer scale, which corresponds to the size of the fluorophore cage. Nevertheless, the closeness of the Stoke shifts observed for chemically distinct polymers drove us to suspect a solvent effect. Indeed, even the air-dried polymer film still contains up to 10% of the solvent. It can therefore be hypothesized that the hydrophobic probe PRODAN would preferentially interact with the xylene solvent. If so, its emission spectrum would mainly reflect the polarity of the solvent used. Two findings confirmed this hypothesis. First, the PRODAN wavelength of maximal emission in xylene is 421 nm, which matches well the values observed in the copolymers. Second, the replacement of xylene by THF for solubilizing the PLAtBu results in a shift from 422 to 438 nm of the PRODAN λ_{max} of emission in this copolymer, value close to that observed in pure THF ($\lambda_{max} = 433$ nm). However, this solvent effect does not invalid the observation that extensive hydration, as observed in PLAtBu, does not alter *on average* the polarity of the polymer matrix since the PRODAN molecule remains in a rather hydrophobic cage from which water is largely, if not totally, excluded.

Effect of Hydration on Copolymer Dynamics. It has been yet suggested that diffusion of water within polymers matrixes was of consequences regarding the polymer dynamics.[21] It was therefore interesting to monitor the moving of chains as the hydration proceeds. Fluorescence anisotropy measurements of PRODAN-labeled copolymers allow to monitor in situ the probe

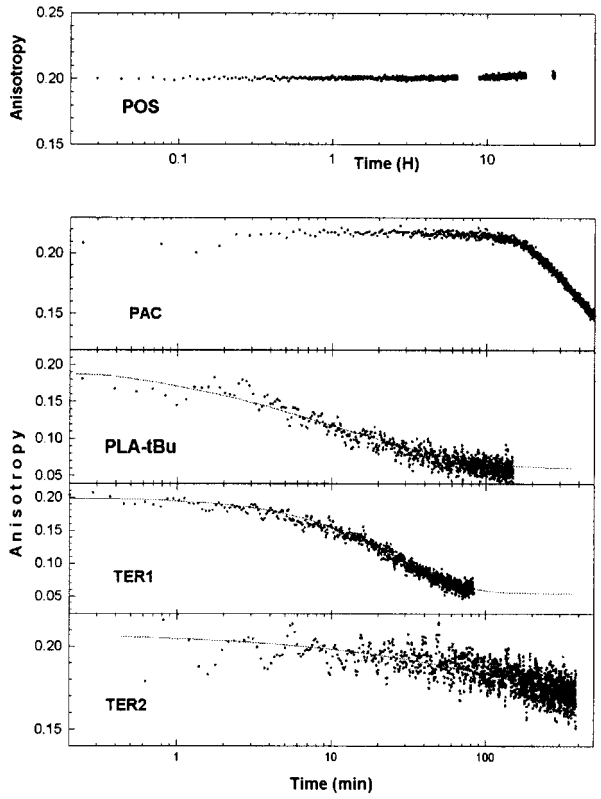

Figure 4. Effect of hydration on the fluorescence anisotropy of PRODAN. PRODAN fluorescence anisotropy is plotted as a function of time with a 350 nm excitation wavelength and a 420 nm emission wavelength. Excitation and emission slits were set to 2.5 nm. Each point is integrated over 30 flashes of the pulsed excitation source. Curve fitting has been applied as indicated in the Experimental section. Continuous lines feature the calculated regression curve. The recovered parameters of the kinetics are displayed in Table 2.

tumbling and hence gives access to polymer dynamics. Indeed, the more constrained the probe, the higher anisotropy. Figure 4 displays the evolution of PRODAN fluorescence anisotropy over time for the five copolymers studied. Except for the POS, for which no variations were observed over 30 h, the decrease of PRODAN fluorescence anisotropy was recorded for up to 6 h. For each sample, it has been checked that no PRODAN release occurs over the time period investigated. This was achieved by collecting the fluorescence in the immersion water after the anisotropy experiments. Only a very weak background fluorescence (less than 1‰ of the total emission) was observed. A common aspect shared by these kinetics is that the initial PRODAN anisotropy is close to 0.2, which indicates that its rotation is highly hindered in the absence of water. This rules out the possibility that the probe was freely rotating in a solvent (xylene) cage in absence of water. Even though it is likely that weak dipole interactions occur between PRODAN and xylene molecules (see above), the probe motions are frizzed due to interactions with the polymer chains. The decrease in anisotropy over time observed in most of the copolymers (see Figure 4) clearly indicates that the chains fluctuations are enhanced as water diffuses. Table 2 summarizes the recovered parameters of the anisotropy time evolutions. As mentioned above, no time-dependent anisotropy variation is observed in POS, indicating that the initial steps of water diffusion have no dynamic consequences in this copolymer. The PAC copolymer exhibits a different pattern, since a lag time of about 100 min is observed before any dynamic change occurs. Then, a pure exponential decay is observed with an apparent decay $\tau \approx 12$ h and a limit value $A_\infty \approx 0.10$. The kinetics observed in the PLAtBu follows a $\sqrt{t}$ stretched exponential law with a decay time τ of 11 min, which indicates that the decrease of PRODAN fluorescence anisotropy is synchronous with the diffusion of water in the matrix. The final anisotropy A_∞ (0.06) is close to that observed for the freely tumbling probe. As mentioned above, it can be ruled out that the probe is released from the polymer in the external water solvent since, first, it is incompatible with the observed maximal wavelength emission (423 nm), and second, no measurable fluorescence was present in the water after the polymer removal. The increased motions of the polymer chains along with the large swelling observed clearly indicate that both the structure and dynamics of the copolymer are drastically altered as a consequence of hydration. The TER1 copolymer exhibits the fastest rate of dynamic changes ($\tau = 9$ min) which does not follow the Fick law since the decay is that of a pure exponential ($\beta = 1$). As observed in the PLAtBu, the observed A_∞ value is very low, this point well matching the apparent high water uptake. Finally, the hydration kinetics of TER2, alike PLAtBu, follows a stretched exponential in $\sqrt{t}$ though the decay is much slower ($\tau = 3.5$ h) than that of PLAtBu; the computed A_∞ value (0.13) suggests that, over the period of time monitored, the hydration process does not induce large fluctuations within the polymer matrix.

Table 2. Evolution with Time of the PRODAN Fluorescence Anisotropy in Hydrated Copolymer[a]

copolymer	$A_{t=0}$	A_∞	lag time	$\sqrt{t}$	τ_{A_f}
POS	0.20	nd	> 30 h	−	nd
PAC	0.21	0.08	≈1.5 h	−	12 h
PLAtBu	0.19	0.06		+	11 min
TER1	0.20	0.06		-	9 min
TER2	0.21	0.13		+	3.5 h

[a] The table summarizes the recovered parameters of the kinetic as the hydration processes. $A_{t=0}$, A_∞, τ_{A_f} featuring the initial anisotropy of PRODAN embedded in the "anhydrous" copolymers, the final recovered anisotropy and the decay time, respectively. In particular cases, lag times are observed before any change in anisotropy occurs. The $\sqrt{t}$ tag indicates whether the kinetics follows a stretched exponential law. nd: not determined.

Structure of Water Dissolved in the Copolymers Matrixes. Besides the kinetic aspects of hydration, attempts have been made to solve the time dependency of the water structure in the copolymers. Since most of the observed kinetics present a bimodal behavior, it may be hypothesized that early events occur before the water sorption significantly increases. The comparative analyses of the water structure at *early* and *late* periods may help in understanding the nature of these events. Hence, the water structure was analyzed at two distinct steps which features its time evolution.

Band decomposition of water ATR−FTIR spectra (Figures 5 and 6 and Table 3) has been performed on the basis of the four-state model[22,23] which takes into account the Raman and IR vibration bands usually observed for water ν_{OH} vibration. The corrected IR spectra have been analyzed in terms of mixed Gauss/Lorentz components. It arises that water components all exhibit a high Gaussian character since the computed Gauss factor was observed between 0.8 and 1 (pure Gaussian) in every case. This discontinuous model

Table 3. Summary of Band Positions, Widths, and Relative Areas for Water ν_{OH} Stretching Modes[a]

band		pure water	POS 8 h/64 h	PAC 8 h/25 h	PLAtBu 30 min/5 h	TER1 26/150 min	TER2 3 h/40 h
A1	ν_0 (cm^{-1})	3630	3609/3627	3604/3629	3628/3627	3591/3591	3597/3597
	$\Delta\nu^{1/2}$ (cm^{-1})	80	159/115	99/135	89/83	108/112	133/208
A2	ν_0 (cm^{-1})	3550	3518/3542	3525/3535	3550/3549	3516/3513	3506/3512
	$\Delta\nu^{1/2}$ (cm^{-1})	155	187/173	194/155	153/146	209/200	169/169
A3	ν_0 (cm^{-1})	3400	3388/3394	3390/3400	3399/3399	3390/3390	3391/3391
	$\Delta\nu^{1/2}$ (cm^{-1})	213	226/221	212/206	216/219	202/200	195/189
A4	ν_0 (cm^{-1})	3232	3216/3220	3225/3229	3225/3225	3237/3236	3233/3235
	$\Delta\nu^{1/2}$ (cm^{-1})	205	194/197	189/196	194/199	188/192	199/ 196

[a] The table presents the recovered parameters from band fitting of ATR-corrected spectra of pure water and water sorpted in the copolymers matrixes. For each copolymer, two spectra have been fitted which correspond to an "early" and "late" stages of hydration. The results here displayed are focused on the evolution of the four ν_{OH} bands even though additional overlapping bands have been taken into account (e.g., ν_{CH} stretching modes) for the fitting process. Typical confidence intervals are $\pm$ 2 cm^{-1} for band positions and $\pm$ 3 cm^{-1} for $\Delta\nu^{1/2}$. See Figure 6 for components relative areas.

describes the state of water as distinct structures which have been assigned to "free" clustered water molecules and to "bound" water molecules interacting with the polymers groups. To help assigning the different structures of water dissolved in the polymer, a comparison has been made with the infrared spectrum of pure water (Figure 5A) collected under similar experimental conditions. The spectral parameters of the four components are displayed in Table 3. According to their positions, they can be ranked from the strength of the H bonding, i.e., band A1, A2, A3, and A4 reflecting very weak (3630 cm^{-1}), weak (3550 cm^{-1}) medium (3400 cm^{-1}), and strong (3232 cm^{-1}) H bonds, respectively. Liquid water (Figure 5A and 6) has its band center near 3375 cm^{-1}, which is close to the A3 maximum (ν_0 = 3400 cm^{-1}) which features 52% of the whole ν_{OH} spectrum area. Hence, this component must reflect the liquid "clustered" water in copolymers.[24] The minor A1 band (ν_0 = 3630 cm^{-1}) reflecting very weak H bonding contributes to 2% of the total area. This band has been assigned to the antisymmetric stretching, ν_3, of water monomers, i.e., water molecules separated from other water molecules and only engaged in relatively weak hydrogen bondings.[24] It has been suggested that this band may also correspond to water dimers weakly bond to a copolymer group.[25] The A2 band (ν_0 = 3550 cm^{-1}) features 11% of the total area and must reflect the symmetric stretching parent of the A1 band. Finally, the A4 band (ν_0 = 3232 cm^{-1}), contributing up to 35% of the envelope, has been assigned to auto-associated water dimers i.e., pairs of water molecules connected by a hydrogen bond in which the overtone of the H_2O bending vibration of one monomer is in Fermi resonance with the OH stretching mode of the parent monomer. Though this four-state discontinuous model of water has not been fully validated, it nevertheless constitutes a realistic model to analyze the structure of water in polymers.

A first approach to study the perturbing effect of the copolymer on water structure is to focus on the relative distribution of water structures (Figure 6). Unsurprisingly, the A1 and A2 components featuring single H bonded molecules are at least equally populated, or are rather more populated, as compared to pure water at the expense of the A3 and A4 component. This is obvious if one looks at TER1 and TER2 for which the A1 and A2 cumulative contribution (Table 3) is twice that observed in pure water after 3 h of hydration, mainly at the expense of the A3 component. As a consequence, the A3 and A4 components featuring "clustered" and water dimers, respectively, are less populated in the various copolymers. It is also to be noted that, except for PAC, the relative contributions of the four components do not drastically vary in the time course of hydration over the time period investigated. This would suggest that, even in the "early" stages of hydration, the water association scheme is not correlated to the water uptake. This general behavior is not observed in the case of PAC since the A2 population is reduced by a 1.7 factor to the benefit of the A3 component as the water content increases about four times. This finding, along with the "S" shaped hydration curve (Figure 3), suggests that structural and dynamic effects occur around 9 h, which are of consequence for the water−polymer interactions.

A second complementary approach for analyzing the water behavior in the copolymers matrixes is to focus on the average energy of the water H bonds (Table 3 and Figure 5). As noted earlier, a commonly observed feature is that water networks are drastically altered in the early steps of hydration, these alterations being reduced as the water content increases. This is shown by early large frequency shifts from the band positions observed in pure water, which tend to vanish later. This effect is particularly drastic for POS or PAC for which the A1 and A2 components significantly upshift (by 18 and 24 cm^{-1} for POS; by 25 and 10 cm^{-1} for PAC), as hydration proceeds. This suggests that strong matrix−water H bonding occurs in the early steps of hydration which weaken at later stages. This behavior is unique to polymer-bound water molecules since the A4 and, to a lesser extent, A3 band positions remain roughly unaltered over the same period of time, hence indicating that the strength of dimers or clustered water H bonds remains roughly unaltered. As underlined above, TER1 and TER2 exhibit large A1 and A2 populations at the expense of the A3 component. Interestingly, this is associated with a drastic downshift of the A1 and A2 bands in these copolymers as compared to pure water: 39 and 37 cm^{-1} and 33 and 38 cm^{-1}, respectively. This clearly indicates that strong water−matrix H bonding occurs within these two hydrophilic copolymers. In the other less hydrophilic or hydrophobic copolymers, both populations and H bondings are close to those observed in pure water. Hence, the water H bonding scheme in a particular copolymer appear to be strongly dependent on the hydrophobic/hydrophilic balance within the matrix.

Polymer Hydration Sites. Besides the analysis of the water network within polymers, attempts have been made to identify the sites of hydration within the copolymers. The most prominent effect of hydration on IR spectra is a time-dependent alteration in the 1750−1600 cm^{-1} frequency domain. This domain encompasses

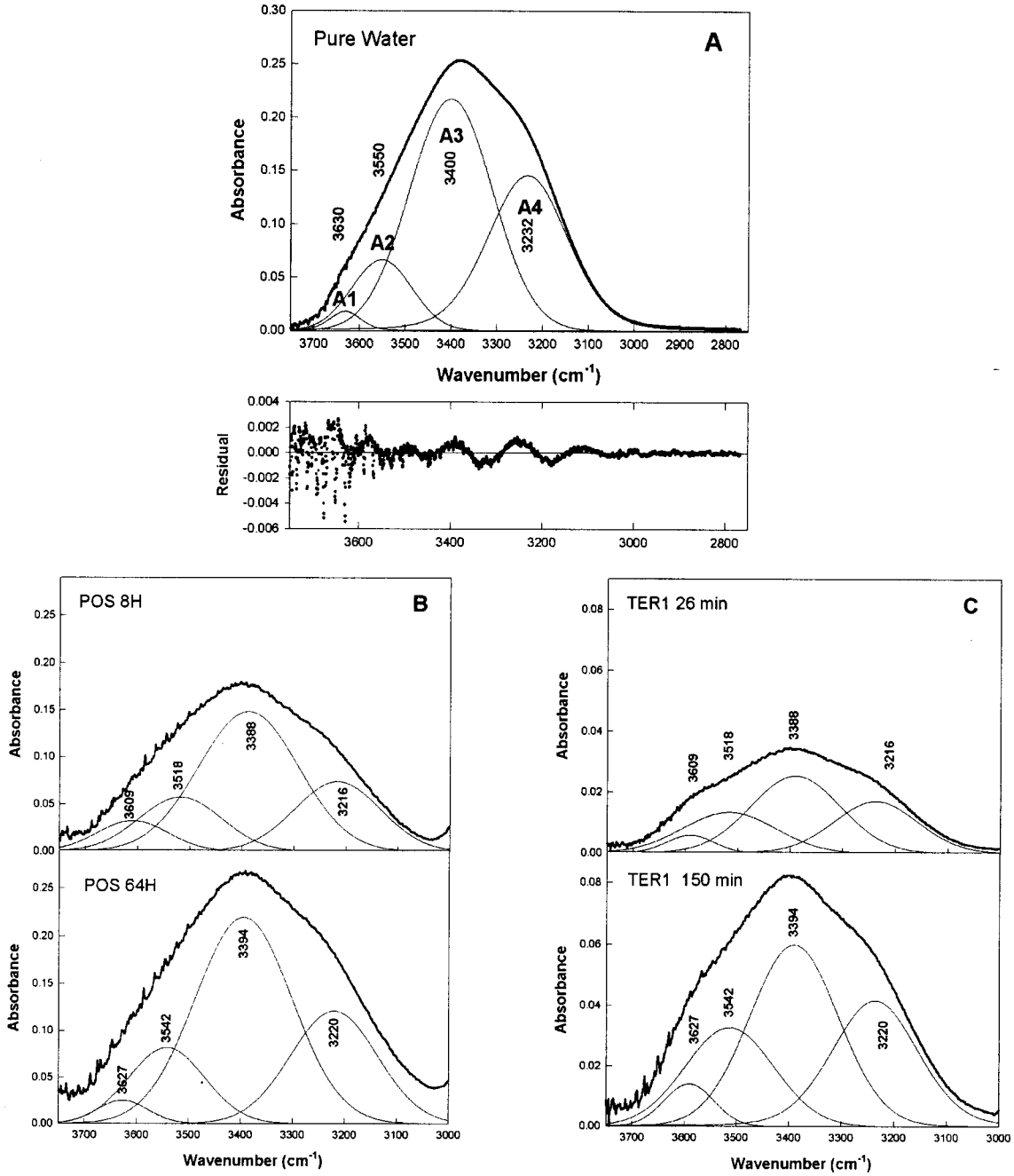

Figure 5. ATR−FTIR spectra of pure water and water dissolved in POS and TER1 copolymers at various stages of hydration. The structure of water dissolved in the various copolymers is analyzed at two stages of hydration by comparison to the IR spectrum of pure liquid water. After correction for ATR induced distortions, band fitting has been used to resolve the four components (A1−A4) of the discontinuous four-state model of water structure. The figure displays the decomposition of the pure liquid water spectrum (A) collected in the same experimental conditions. As a matter of example, water ν_{OH} IR spectra in POS (B) and TER1 (C) are displayed. Each component has been fitted assuming a mixed Gaussian/Lorentzian band shape in terms of band position (ν^0), intensity, full width at half-height ($\Delta\nu^{1/2}$) and Gauss fraction. In every case, components exhibit a high (>0.8) Gauss factor. The corresponding computed parameters are displayed in Table 3.

the copolymers carbonyl and carboxyl stretching modes along with the water δ_{OH} bending vibration located at 1636 cm^{-1}. In this domain, the copolymers vibrational bands were assigned by comparison to ATR−FTIR spectra of monomers (data not shown). The assignment of these groups are summarized in Table 4. As a matter of example Figure 7 shows the POS- and TER1-corrected ATR−FTIR spectra in this frequency domain. For each copolymer, a first "anhydrous" spectrum was collected prior to water addition, and then, "hydrated" spectra were sequentially collected to investigate the effect of hydration on the $\nu_{C=O}$ groups. A general characteristic is that no significant shift occurs during the hydration, but instead, it is the relative contribution of the bands which is altered. For all polymers but TER2, it is observed that as the water δ_{OH} band increases, the copolymers $\nu_{C=O}$ bands located around 1730−1750 cm^{-1} decrease at the expense of the ≈1710 cm^{-1} band. This inverse correlation indicates that the carbonyl groups, not initially engaged in hydrogen bonds, progressively contract H bonding ($\nu_{C=O\cdots}$) with an increasing number of water molecules and, hence, downshift. Hence, in these copolymers, the main class of binding sites for water are the C═O polar groups

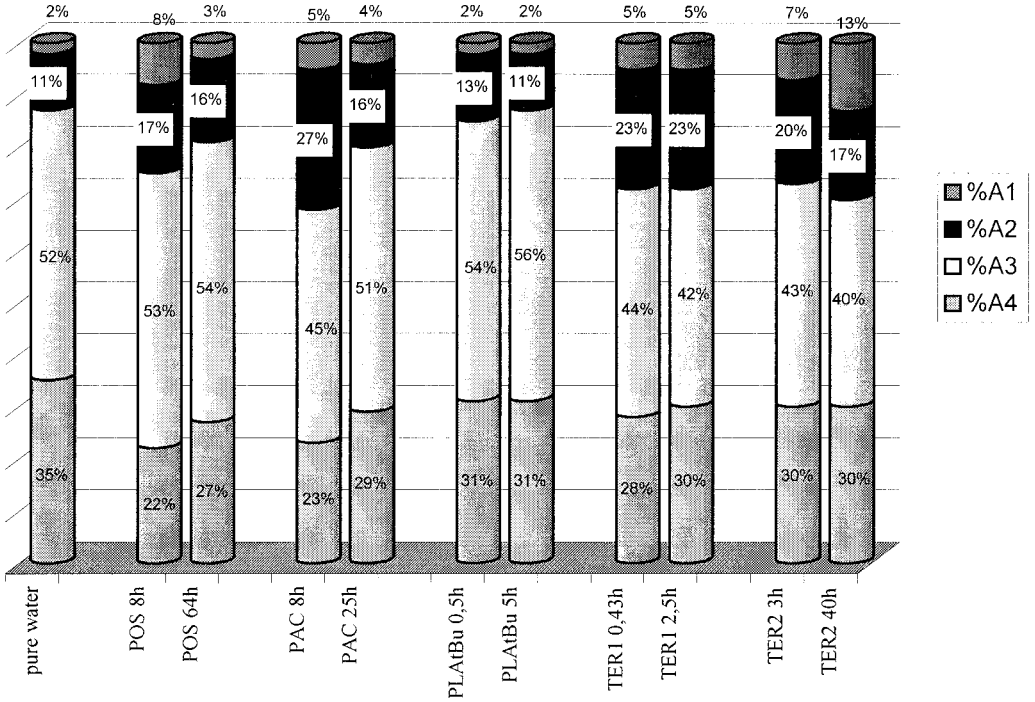

Figure 6. Relative contributions of the four bands corresponding to νOH of pure water and water absorbed in polymers.

Table 4. Assignment of Monomers Vibrational Bands in the 1800−1600 cm^{-1} Frequency Domain[a]

monomer	vibration (cm^{-1})	assignment	copolymer
methyl methacrylate	1729	$\nu_{C=O}$	POS − PAC
tributyltin methacrylate	1729	$\nu_{C=O}$	POS
butyl methacrylate	1729	$\nu_{C=O}$	PAC
tBu	1723	$\nu_{C=O}$	TER1−TER2−PLAtBu
DMAM	1720	$\nu_{C=O}$	TER1−TER2
HPA	1724	$\nu_{C=O}$	TER1
TPA	1755	$\nu_{C=O}$	TER2
PLA	1754	$\nu_{C=O}$	PLAtBu
rosin	1696	ν_{COOH}	PAC

[a] Vibrational stretching modes in copolymers have been assigned from the vibrations observed in the constitutive monomers in the 1800−1600 cm^{-1} frequency domain.

involved in the main chains esterification. It is likely, that, as observed in other copolymers,[26] each adsorbed water molecule may interact with two of these groups. Besides, the general occurrence of a more or less populated $\nu_{C=O}$··· band in "anhydrous" spectra likely arises from the presence of residual water molecules retained in the copolymers matrixes. In the case of the PLAtBu copolymer, the $\nu_{C=O}$ bands assignments allow one to establish that tBu carbonyl groups are preferentially hydrated since the corresponding band (1726 cm^{-1}) is selectively reduced by 20% after 1 h of hydration whereas the 1750 cm^{-1} band (PLA) remains roughly unaltered. For the two copolymers, PAC and TER2, which exhibit the slowest hydration process (see Figure 3), it is interesting to note that the sole PAC exhibits an increase in H bonding over the period investigated. The corresponding "late" stage (23 h), being located beyond the "S" shape transition observed, let one hypothesize that the now evoked early events must constitute an absolute prerequisite for the hydration of the copolymer's binding sites. On the opposite side, the carbonyl groups of the TER2 copolymer, for which

Table 5. Spectral Analysis of Anhydrous and Hydrated Copolymers in the Carbonyl Stretching Frequency Domain[a]

copolymer	POS	PAC	PLAtBu	TER1	TER2
immersion duration	0/70 h	0/23 h	0/60 min	0/80 min	0/50 H
peak assignment					
$\nu_{C=O}$ (cm^{-1})	1733/1733	1731/1731	1726/1727	1729/1726	1724/1724
$\Delta\nu^{1/2}$ (cm^{-1})	20/21	24/25	37/33	18/21	23/24
area (%)	72/61	43/45	55/34	66/59	59/60
$\nu_{C=O}$ (cm^{-1})			1750/1752		1767/1766
$\Delta\nu^{1/2}$ (cm^{-1})			32/31		21/22
area (%)			29/30		39/38
ν_{COOH} (cm^{-1})		1695/1693			
$\Delta\nu^{1/2}$ (cm^{-1})		24/23			
area (%)		47/40			
$\nu_{C=O}$··· (cm^{-1})	1715/1712	1716/1708	1703/1701	1711/1711	1709/1708
$\Delta\nu^{1/2}$ (cm^{-1})	32/42	19/18	32/43	27/18	9/9
area (%)	28/39	10/15	16/36	34/41	2/2
δ_{OH} (cm^{-1})	1638/1639	1656/1646	1655/1640	-/1652	1643/1644
$\Delta\nu^{1/2}$ (cm^{-1})	59/65	93/97	96/87	-/102	132/148
area (cm^{-1})	11.31/17.8	3.09/7.32	6.04/8.08	-/2.23	6.25/16.4

[a] IR spectra of the copoylmers have been fitted in the 1800−1500 cm^{-1} frequency domain prior and after addition of water in excess. $\nu_{C=O}$ and $\nu_{C=O}$··· peaks feature free and H bonded carbonyl groups, respectively. The rosin ν_{COOH} vibration also shows up in the PAC IR spectrum. Relative areas (%) are only calculated for carbonyl and carboxyl components. Hence, the extent of H bonding can be deduced from the relative contribution of the $\nu_{C=O}$··· band. Water δ_{OH} areas are displayed in cm^{-1}.

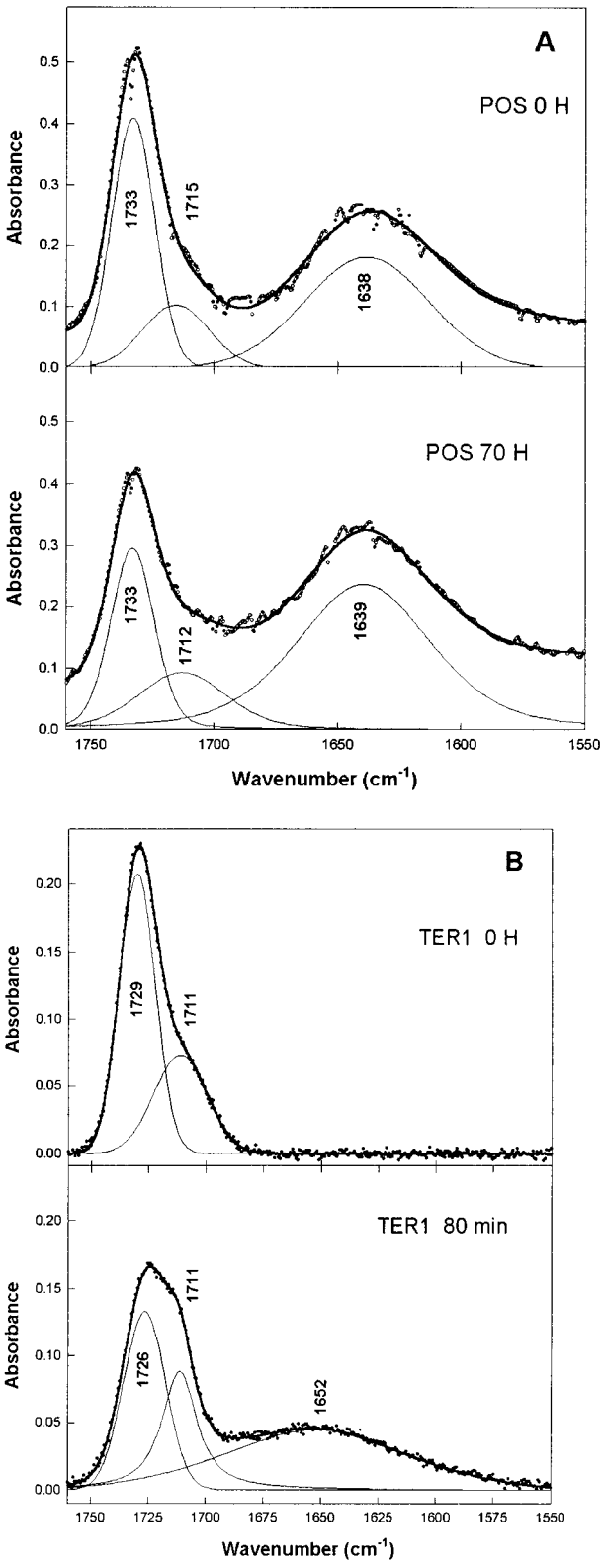

Figure 7. Effect of hydration on the carbonyl groups hydrogen bonding. Sequentially collected IR spectra of copolymers are displayed in the 1760−1550 cm^{-1} frequency domain under the same experimental conditions as in Figure 5. For example, band fitting of POS (A) and TER1 (B) copolymers are displayed. The first spectrum is collected prior to water addition, the second at a later stage and features the hydrated polymer. Band assignment derives from comparison of the observed IR polymer spectra with those of monomers (see Table 4). The recovered parameters are displayed in Table 5. The $\nu_{C=O}$ and ν_{COOH} bands exhibit Gauss factors in the 0.7−1 range whereas the δ_{OH} band exhibits a pure Gaussian character.

hydration kinetics is monotonic, remain unaltered after a 50 h period of immersion. Since this copolymer contains tBu groups which exhibit fast H bonding in the PLAtBu copolymer, it arises that not only the chemical nature of the acceptor but also the polymer matrix plays a prominent role in the water accessibility to potential binding sites. The low chain fluctuations observed in this copolymer may certainly contribute to this effect.

Conclusion

The molecular design of erodable polymers allowing the controlled release of biocides requires deep insights into the phenomena which occur *prior* to hydrolysis, this is to say the hydration. Accordingly, the present study aims to bring to the fore the structural and dynamic aspects of the early stages of hydration in polymers of interest. Two distinct and complementary techniques have been used to monitor in situ the diffusion of water molecules within the polymer matrix, fluorescence and infrared spectroscopies. These techniques are powerful since they allow to simultaneously probe the mode (Fickian or non-Fickian) of diffusion, the kinetics of water sorption, the chains fluctuations, the H bonds networks, and the water binding sites.

The FTIR−ATR structural analysis of the water dissolved in the polymers clearly shows that the five copolymers here investigated exhibit distinctive patterns of hydration both by the amount of water sorpted and the mode of diffusion. In most of the cases, bimodal hydration kinetics are observed, suggesting thereby that early events occur as a consequence of the diffusion of water. This point is also confirmed by the fluorescence anisotropy experiments which also establish, for the first time, a direct link between the diffusion of water and the dynamics of the polymer chains. Here again, if one looks at the POS behavior, no single idealistic behavior is observed since this copolymer undergoes a significant water uptake without any concomitant change in the chains fluctuations.

In the limit of validity of the discontinuous four-state model of water structure, we are also be able to discriminate "bound" from "free" water and to investigate the average energy of the different bonding schemes. The unevoked perturbing effect of the matrix on the water networks can hence now be investigated. Moreover, the involvement of the carbonyl groups of the polymers in the hydration process is clearly assessed in this study. These groups must consist of water high affinity acceptors whose H bonds are featured in the A1 and A2 components of the ν_{OH} IR spectra. This assumption is further supported by the comparison of the ν_{OH} and $\nu_{C=O}$ kinetics: the faster the hydration proceeds, the faster the $\nu_{C=O}$ high frequency, i.e., unbound, components vanish. This finding allows to assess a relation between the hydration kinetic and the formation of H bonds with the polymer carbonyl groups. A deeper investigation of their IR spectra should help to tackle the dynamical accessibility of the water to these binding sites which must rely on the polymer morphology. On the other hand, no correlation was observed between the hydrophilicity of the polymer and the kinetic of H bonds formation. Indeed, though TER1 and TER2 are both considered as hydrophilic, they do exhibit distinctive behaviors since early intermolecular H bonding is only observed in TER1.

As recalled in the Introduction, the hydrolysis within the macromolecular chains is a complex phenomenon

which still requires extensive investigation. The growing development of noninvasive techniques allowing one to monitor in situ structural, dynamic, and energetic parameters will be of great help in solving the cross-disciplinary enigma of polymer hydration.

Acknowledgment. The authors are greatly indebted to Pr. François Gaillard for his interest and critical review of the paper and to Y. Hemery for his technical assistance. We also greatly acknowledge La Région Bretagne for the financial support of M.T.

References and Notes

(1) Langer, R. *Nature* **1998**, *5*, 392.
(2) Ritger, P. L.; Peppas, N. A. *J. Controlled Release* **1987**, *5*, 37.
(3) Adrover; Giona, M.; Grassi, M. *J. Membr. Sci.* **1996**, *113*, 21.
(4) Muller, M.; Schmitt, F. J. *Macromol. Symp.* **1997**, *119*, 269.
(5) Vallée-Rehel, K.; Mariette, B.; Hoarau, P. A.; Guerin, P. *Analysis* **1998**, *26*, 1.
(6) Vallée-Rehel, K.; Langlois, V.; Guerin P. *J. Environ. Polym. Degrad.* **1998**, *6*, 175.
(7) Siparsky, G. L.; Voorhees, K. J.; Dorgan, J. R.; Schilling, K. *J. Environ. Polym. Degrad.* **1997**, *5*, 125.
(8) Ross, R. J.; Batzel, D. A.; Meah, A. R.; Kneller, J. F. *Macromol. Symp.* **1997**, *123*, 235.
(9) Vallée-Réhel, K.; Mariette, B.; Hoarau, P. *Eur. Polym. J.* **1998**, *34*, 683.
(10) Vallée-Réhel, K.; Langlois, V.; Guérin, P.; Leborgne, A. *J. Environ. Degrad.* **1999**, *7*, 27.
(11) Cameron, D. G.; Moffatt, D. J. *Appl. Spectrosc.* **1987**, *41*, 539.
(12) Dong, H. P.; Caughey, W. S. *Biochemistry* **1990**, *29*, 3303.
(13) Hasinoff, B. B. *J. Phys. Chem.* **1978**, *82*, 2630.
(14) Iben, I. E. T.; Braunstein, D.; Doster, W.; Frauenfelder, H.; Hong, M. K.; Johnson, J. B.; Luck, S.; Ormos, P.; Schulte, A.; Steinbach, P. J.; Xie, A. H.; Young, R. D. *Phys. Rev. Lett.* **1989**, *62*, 1916.
(15) Koenig, J. L.; Weisenberger L. A. *Appl. Spectrosc.* **1989**, *43*, 1117.
(16) Thomas, N. L.; Windle, A. H. *Polymer* **1981**, *22*, 627.
(17) Hui, C. Y.; Wu, K. C.; Lasky, R. C.; Kramer, E. J. *J. Appl. Phys.* **1987**, *61*, 5129.
(18) Sutandar, P.; Ahn, D. J.; Franses, E. I. *Macromolecules* **1994**, *27*, 7316.
(19) Weber, G.; Farris, F. J. *Biochemistry* **1979**, *18*, 3075.
(20) Macgregor, R. B.; Weber, G. *Nature* **1986**, *319*, 70.
(21) Linossier, I.; Gaillard, F.; Romand, M.; Feller, J. F. *J. Appl. Polym. Sci.* **1997**, *66*, 2465.
(22) Maeda, Y.; Kitano, H. *Spectrochim. Acta, Part A* **1995**, *51*, 2433.
(23) Sammon, C.; Mura, C.; Yarwood, J. *J. Phys. Chem B* **1998**, *102*, 3402.
(24) Toprak, C.; Agar, J. N.; Falk, M. *Trans. Faraday Soc.* **1979**, *1*, 803.
(25) Kusanagi, M.; Yukawa S. *Polymer* **1994**, *35*, 5637.
(26) Berendsen, H. J. C.; *Water: A comprehensive Treatise*; Franks, F., Ed.; Plenum Press: London, 1975; pp 293, 5.

MA010501K